Radionuclide wiggle-matching reveals a non-synchronous Early Holocene climate oscillation in Greenland and Western Europe around a grand solar minimum

Florian Mekhaldi[1], Markus Czymzik[2], Florian Adolphi[1,3], Jesper Sjolte[1], Svante Björck[1], Ala Aldahan[4], Achim Brauer[5], Celia Martin-Puertas[6], Göran Possnert[7], and Raimund Muscheler[1]

[1]Department of Geology - Quaternary Sciences, Lund University, 22362Lund, Sweden
[2]Leibniz-Institute for Baltic Sea Research Warnemünde (IOW), Marine Geology, 18119 Rostock, Germany
[3]Physics Institute, Climate and Environmental Physics & Oeschger Centre for Climate Change Research, University of Bern, 3012 Bern, Switzerland
[4]Department of Geology, United Arab Emirates University, 15551 Al Ain, UAE
[5]GFZ-German Research Centre for Geosciences, Climate Dynamics and Landscape Evolution, 14473 Potsdam, Germany
[6]Department of Geography, Royal Holloway University of London, Egham, Surrey TW20 0EX, UK
[7]Tandem Laboratory, Uppsala University, 75120 Uppsala, Sweden

Correspondence to: Florian Mekhaldi (florian.mekhaldi@geol.lu.se)

Abstract. Several climate events have been reported from the Early Holocene superepoch, the best known of these being the Preboreal oscillation (PBO). It is still unclear how the PBO and the number of climate events observed in Greenland ice cores and European terrestrial records are related to one another. This is mainly due to uncertainties in the chronologies of the records. Here, we present new high resolution ^{10}Be concentration data from the varved Meerfelder Maar sediment record in Germany, spanning the period 11,310-11,000 years BP. These new data allow us to synchronize this well-studied record as well as Greenland ice-core records to the IntCal13 time-scale via radionuclide wiggle-matching. In doing so, we show that the climate oscillations identified in Greenland and Europe between 11,450 and 11,000 years BP were not synchronous but terminated and began, respectively, with the onset of a grand solar minimum. A similar spatial anomaly pattern is found in a number of modeling studies on solar forcing of climate in the North Atlantic region. We further postulate that freshwater delivery to the North Atlantic would have had the potential to amplify solar forcing through a slowdown of the Atlantic meridional overturning circulation (AMOC) reinforcing surface air temperature anomalies in the region.

1 Introduction

One of the great challenges in paleoclimatology today is to better assess the spatial and temporal dynamics of past climate changes. This can only be achieved through robust and consistent chronologies for different records and different regions. Unfortunately, this is a challenging task and we often assume synchrony of such events by climate-tuning different records. One such example is the Preboreal oscillation (PBO) (Björck et al., 1996) and represents a cold spell which occurred shortly after the Younger-Dryas/Holocene transition. Indications of a cold phase have also been reported in a number of European terrestrial records, most of which use biological proxy and isotope data (Björck et al., 1996; Björck et al., 1997; Bos et al., 2007; Magny et al., 2007, van der Plicht et al., 2004; von Grafenstein et al., 1999). A cold and dry climate oscillation, thought to be related to the European PBO, has also been observed in the $\delta^{18}O$ and accumulation signals of a number of Greenland ice cores between 11,520-11,400 years before AD 2000 (b2k) and referred to as the 11.4 ka event (Rasmussen et al., 2007; 2014). Due to chronology uncertainties, it is however unclear whether the 11.4 ka event in Greenland and the European PBO represent one single and synchronous widespread event, an event that spread over time, or whether the European PBO is unrelated to the 11.4 ka event in Greenland. These open questions limit our understanding of the underlying mechanisms of these climate changes.

Around this period, one of the largest and the longest-lasting grand minimum in solar activity of the Holocene occurred between 11,280-10,960 years before AD 1950 (BP). This was evidenced by beryllium-10 (^{10}Be) data in the GISP2 and GRIP ice cores in central Greenland (Finkel and Nishiizumi, 1997; Muscheler et al., 2004; Adolphi et al., 2014) and by $\Delta^{14}C$ ($^{14}C/^{12}C$ corrected for fractionation and decay, relative to a standard, and noted as Δ in Stuiver and Polach (1977)) derived from tree rings (Reimer et al., 2013). This substantial change in solar activity (from high to persistently low) offers an advantage to us for synchronizing time-scales as it has left a clear imprint on the atmospheric production rate of the cosmogenic radionuclides ^{10}Be and ^{14}C. That is, these radionuclides are produced by a nuclear cascade that is triggered when cosmic rays enter the atmosphere. The Earth is shielded, to some extent, from these cosmic rays by the fluctuating strength of the helio- and geomagnetic fields. Therefore, radionuclides carry in part the signal of solar activity, which is then stored in natural archives such as in polar ice caps or lake sediments (^{10}Be) as well as in tree rings (^{14}C). In consequence, we can use these global fluctuations in atmospheric production rate of radionuclides to synchronize records from different environmental archives and investigate the timing of climate events during the earliest part of the Holocene (Southon, 2002; Muscheler et al., 2014; Adolphi and Muscheler, 2016).

Here we present new high-resolution ^{10}Be concentration measurements from the well-studied varved Meerfelder Maar sediment record (MFM) in western Germany, spanning across these large fluctuations in solar activity from 11,310 to 11,000 years BP. Because of its limited catchment area and the existence of ^{10}Be data covering the Late Glacial-Holocene transition (Czymzik et al., 2016), MFM represents an ideal location for the aim of this study. As such, the new ^{10}Be data allow us to synchronize the MFM and Greenland ice core records with the IntCal13 time-scale through wiggle-matching of these different radionuclide records. We can then investigate the timing of the fluctuations observed in the corresponding paleoclimate records at a high chronological precision and assess their relationship in regard to changes in solar activity.

2 Methods

2.1 Preparation of sediment ^{10}Be samples

The new ^{10}Be samples come from the composite sediment profile MFM09 (Martin-Puertas et al., 2012a) which was retrieved at MFM, a deep crater lake situated in the Eiffel region in western Germany that is annually laminated (varved) throughout most of the Holocene (Brauer et al., 2000). About 0.25 g of dried and crushed material was taken for each sample with a temporal resolution of 3 and 10 years (see dataset in Sup. Info.) and 0.5 mg of ^{9}Be carrier was added. ^{10}Be was extracted from the sediment samples at the ^{10}Be laboratory of the Earth Sciences Department of Uppsala University, Sweden, following the methodology described by Berggren et al. (2010). All samples were measured using the Accelerator Mass Spectrometer (AMS) of the Tandem laboratory in Uppsala. The ^{10}Be concentration (in atoms/g) of each sample is calculated based on the ^{10}Be counts R to ^{9}Be counts Rst ratio and taking in consideration the NIST SRM 4325 reference standard (^{10}Be/^{9}Be = 2.68 10^{-11}), the weights of the carrier W_C and of the sample W_S as well as the Avogadro constant N_A and atomic weight A_r of beryllium:

$$^{10}Be\ conc. = \frac{R}{R_{st}} * 2.68\ 10^{-11} * \frac{W_C}{W_S} * \frac{N_A}{A_r}$$

2.2 Chronologies and synchronization

The paleoclimate data investigated henceforth come from different studies, with different records and thus different chronologies. The new sediment ^{10}Be concentration data come from MFM, the chronology of which (MFM2012) was established using mainly microscopic varve counting fixed on an absolute time-scale via tephrochronology as well as radiocarbon dating with a maximum varve counting error of up to 110 years (Brauer et al., 2000; Martin-Puertas et al., 2012a). A more recent chronology (MFM2015) exists which includes the identification and age of the Vedde Ash although it remains unchanged for the Holocene part (Lane et al., 2015), which is the period of focus in this study. We also use published ^{10}Be data (Adolphi et al., 2014) from the GRIP ice core in central Greenland and within the Greenland Ice Core Chronology (GICC05) framework (Rasmussen et al., 2006; Vinther et al., 2006; Svensson et al., 2008; Seierstad et al., 2014). Finally, we use ^{14}C production rate data (Muscheler et al., 2014) inferred from the IntCal13 ^{14}C calibration curve (Reimer et al., 2013) as the anchoring record for our synchronization. That is, we synchronize the MFM2012 time-scale (using our ^{10}Be concentration data) as well as the GICC05 time-scale (using the GRIP ^{10}Be concentration data) to IntCal13 (using the ^{14}C production rate data).

The synchronization of the different radionuclide records was computed following the methodology described by Adolphi and Muscheler (2016). For these calculations we linearly detrend all radionuclide records between 11,000 and 11,800 years BP and assumed a production rate uncertainty of 20% for all records, which corresponds to the root mean square error between the records after synchronization.

3 Results

3. 1 Meerfelder Maar [10]Be concentrations

The new [10]Be concentration measurements from MFM are displayed in Fig. 1, alongside with [10]Be concentrations from the GRIP ice core in central Greenland (Finkel and Nishiizumi, 1997; Muscheler et al., 2004; Adolphi et al., 2014), and with older [10]Be concentration data from MFM for the Late Glacial-Holocene transition (Czymzik et al., 2016). Each dataset is plotted on its original time-scale – that is, the MFM2012 chronology (Brauer et al., 2000; Martin-Puertas et al., 2012a) and the GICC05 chronology (Rasmussen et al., 2006; Vinther et al., 2006; Svensson et al., 2008; Seierstad et al., 2014). The most striking feature of these datasets is the approximately 250-year long period of increased [10]Be concentration around 11,150 years BP. The most likely explanation for this increase is a decrease in the intensity of the heliomagnetic field (solar activity) leading to an increased impingement of Earth by galactic cosmic rays and thus, an increased atmospheric production rate of [10]Be and ^{14}C nuclides. It was also shown that meteorological and catchment influences on [10]Be deposition are likely small at MFM (Czymzik et al., 2016). The high resolution of our [10]Be measurements allows us to observe finer structures within this period of increased [10]Be concentration. One example is the double peak structure at 11,040 and 11,200 years BP, which is also present in ^{14}C atmospheric production rate data (Muscheler et al., 2014), but not well-expressed in the GRIP [10]Be data. Finally, it is of importance to note that although the increased production around 11,150 years BP is observed in all these radionuclide records, there is an apparent chronology offset at its onset around 11,300 years BP (Fig. 1). More specifically, the [10]Be concentration data from GRIP begin to increase around 11,320 years BP whereas a similar increase is seen in the [10]Be concentration from MFM about a hundred years later.

3. 2 Time-scales synchronization

The Greenland ice core time-scale is characterized by an accumulating layer counting uncertainty back in time (Rasmussen et al., 2006) as are chronologies based on sediment varve counting such as MFM. In comparison tree ring chronologies, underlying the ^{14}C calibration record, are considered accurate with virtually no dating uncertainty for the Holocene period (Reimer et al., 2013). Considering the different time-scale uncertainties, it is challenging to compare the timing of short-lived climate oscillations such as the PBO/11.4 ka event. Here we use the global signature common to all cosmogenic radionuclide records as a synchronization tool (Muscheler et al., 2008; 2014). More specifically, we use the large fluctuations in both the MFM and GRIP [10]Be data to synchronize these records onto the chronologically more accurate and precise IntCal13 time-scale (Czymzik et al., 2018). It was previously shown that GICC05 increasingly overestimates age during the Holocene, compared to IntCal13 (Muscheler et al., 2014) and this time-scale difference is estimated to increase to 67 (± 6) years at 11,000 years BP (Adolphi and Muscheler, 2016). We use the same Bayesian wiggle-matching approach as in Adolphi and Muscheler (2016), but here for the period 11,000-11,800 years BP to synchronize both the MFM sediment and Greenland ice core records onto IntCal13.

Figure 2 shows both the ice-core and sediment-core [10]Be data once synchronized onto the IntCal13 time-scale using the ^{14}C production rate from Muscheler et al. (2014), with the corresponding probability density functions displayed on the right-hand panel. We find that the MFM [10]Be data fit best with ^{14}C by adding 20 years

152 to MFM2012 (+6/-19 years uncertainty with a 95.4% confidence interval), whereas the GRIP [10]Be data fit best

153 with ^{14}C by shifting GICC05 78 years towards present (+32/-8 years uncertainty with a 95.4% likelihood

154 interval). When comparing GICC05 directly to MFM2012, we find that the best fit occurs by shifting GICC05

155 72 years towards MFM2012 (+4/-8 years with a 95.4% likelihood interval). There is thus a difference of 26

156 years (72 +4/-8 years vs. 98 +33/-21 years) when comparing GICC05 and MFM2012 directly, rather than

157 synchronizing them to IntCal13 first which illustrates the uncertainties inherent to this exercise. In the following,

158 we will compare GICC05 and MFM2012 when synchronized to IntCal13 as it is the more robust time-scale and

159 thus consider the combined chronology offset of 98 (+33/-21) years. Another uncertainty from these estimates

160 arises from the influence of climate on the cosmogenic signal of all radionuclides (Adolphi et al., 2014;

161 Muscheler et al., 2008; Pedro et al., 2012). For instance, ^{14}C oxidizes to form [14]CO_2 and enters the carbon cycle

162 while [10]Be readily attaches to aerosols and is thus influenced by precipitation. Even though [10]Be deposition is not

163 expected to have strong environmental influences at MFM (Czymzik et al., 2016), this was taken into account

164 within the 20% uncertainty since these effects are difficult to quantify objectively.

165

166 **3.3 Anomalies in paleoclimate proxies between 11,450-11,000 years BP**

167 If we correct the GICC05 and MFM2012 timescales for their respective offsets to IntCal13, we can compare

168 Early Holocene climate in Greenland to data from MFM with a high chronological precision. Figure 3 displays a

169 selection of climate proxies from both Greenland ice cores and the varved MFM record on the IntCal13 time-

170 scale, as per Fig. 2. In addition, both ^{14}C atmospheric production rate and GRIP [10]Be concentrations are shown

171 as a general indicator of changes in solar activity (Fig. 3a). The stack of $\delta^{18}O$ anomalies from four Greenland ice

172 cores (DYE-3, GRIP, NGRIP, and Renland - Fig. 3b) can be related to surface air temperature around Greenland

173 (Rasmussen et al., 2007; Vinther et al., 2009) and shows one negative fluctuation between 11,400-11.250 years

174 BP. Following this oscillation, the Greenland $\delta^{18}O$ anomaly record remains largely constant and positive. In

175 addition, we also use the accumulation rate anomaly stack (Fig. 3c) from the DYE-3, GRIP, and NGRIP ice

176 cores (Rasmussen et al., 2007) to illustrate changes in snow accumulation rates over Greenland. Here again, a

177 negative fluctuation is observed between 11,400-11.250 years BP. Then, we make use of the MFM δD records

178 of n-alkanes (Fig. 3d) that has been interpreted as a proxy for precipitation δD (Rach et al., 2014) which,

179 similarly to $\delta^{18}O$ in Greenland, can thus be regarded as indicative of distance from, and temperature/humidity at

180 the moisture source (Dansgaard, 1964) as well as fractionation related to air temperature. As opposed to the

181 Greenland stack, the δD data show no fluctuations between 11,400-11,250 years BP with δD_{aq} remaining

182 constant and δD_{terr} showing an increasing trend. Then at 11,250 years BP, both δD series depict a 20% drop that

183 persists until 11,100 years BP. To test the spatial scale to which the δD record from MFM can be representative

184 of, we have investigated the spatial relationship between surface air temperature (SAT) in the NOAA-CIRES

185 20th climate reanalysis V2c (20CR; Compo et al., 2011) and δD in precipitation from the Trier meteorological

186 station (about 50 km SW of MFM). It can be seen from Fig. 4 that there is a significant relationship (p <0.1)

187 between annual precipitation δD from the Trier station (IAEA/WMO, 2006) and annual SAT over most of

188 western Europe. In addition, Fig. 4 also points to a relationship between annual SATs over Greenland-Iceland

189 and annual $\delta^{18}O$ at Summit (Steig et al., 1994; White et al., 2009). Finally, we also show varve thickness changes

190 at MFM that were primarily controlled by runoff from the catchment. After a period of low varve thickness, a

sharp increase occurred 11,250 years BP followed by a gradual decrease and a second but very small increase around 11,080 years BP. Titanium centered-log ratio data (Ti_{clr}), determined by micro X-ray fluorescence (μ-XRF) from the same MFM sediment composite profile (Martin-Puertas et al., 2017), confirm the interpretation that the variance in varve thickness at the time was mostly controlled by detrital supply to the lake (Fig. 3e). It is important to mention that on a longer time perspective, the changes described above in the sediments of MFM (Martin-Puertas et al., 2017; Rach et al., 2012) do not exceed other fluctuations in varve thickness and Ti_{clr}.

4 Discussion

4.1 Timing and interpretation of anomalies between 11,450-11,000 years BP

In Greenland, a cold and dry climate episode occurred around 11,400-11,250 years BP known as the 11.4 ka event (Rasmussen et al., 2007). This is evidenced by a significant drop in the signal of the Greenland ice core $\delta^{18}O$ stack as well as in the accumulation stack (Fig. 3b-c). By shifting GICC05 78 years towards present, this means that the central part of the 11.4 ka event (lowest value in $\delta^{18}O$) is dated to about 11,372-11,272 (+32/-8) years BP which is consistent with GICC05 within the combined uncertainty of our synchronization and the maximum counting error in GICC05. When looking at the temperature proxy and varve thickness from MFM (Fig. 3d-e), we do not find any event that is coeval with the 11.4 ka event in Greenland. Interestingly though, Ti_{clr} data (Fig. 3e) gradually decreased from ca. 11,490 years BP only to be interrupted by a small increase around 11,300 years BP. The low Ti_{clr} data suggest less runoff probably related to drier conditions. Therefore, a possible link to the dry "Rammelbeek Phase" described from the Borchert peat sequence in the Netherlands (van der Plicht et al., 2004; Bos et al., 2007) may be tentatively put forward although chronological uncertainties hinder proving this. We can now also confidently deduce that the termination of the $\delta^{18}O$ and accumulation anomalies in Greenland (the 11.4 ka event) is synchronous with a large decrease in solar activity (Fig. 3a-c). More specifically, high levels of solar activity prevailed throughout the occurrence of the 11.4 ka event in Greenland. Then as solar activity started to decrease (circa 11,250 years BP) into a grand solar minimum that lasted for about 250 years, climate in Greenland switched back to warmer and wetter conditions with higher $\delta^{18}O$ values and accumulation rate. This is in accordance with the suggestion of an abrupt warming (4° ±1.5°) in Greenland following the event, based on $\delta^{15}N$ in the GIPS2 ice core (Kobashi et al., 2008). The rapid transition towards positive accumulation anomalies occurred over a few decades only.

While climate over Greenland following the 11.4 ka event returned rapidly to warmer and wetter conditions, all proxies from MFM sediments (Fig. 3d-e) show fluctuations around 11,250 years BP (henceforth MFM oscillation). In particular, aquatic δD data from small-chain alkanes (Rach et al., 2014) show a clear oscillation with a 20% drop around 11,250 years BP (Fig. 3d) while terrestrial δD data show a decrease reaching levels seen about 11,500 years BP. This deuterium depletion in the alkanes most likely mirrors a depletion of deuterium in precipitation which can be explained, in part, by lower air temperatures over western Europe in view of Fig. 4. Simultaneously, varve thickness and Ti_{clr} show a rapid increase at 11,250 years BP (Fig. 3e) denoting a likely increasing detrital contribution to this varve thickening. When considered into a longer time perspective (Martin-Puertas et al., 2017), this varve increase reaches the level of other fluctuations that are unrelated to known Early Holocene oscillations in North-Atlantic climate. Nevertheless, this shift at 11,250 year

229 BP does correspond to a change in the composition of the sediments as Martin-Puertas et al. (2017) defined a
230 compositional boundary of MFM varves at 11,230 years BP (11,250 years BP on the IntCal13 time-scale), based
231 on µ-XRF scanning analyzed with Ward's clustering methods. By synchronizing MFM2012 onto IntCal13 (Fig.
232 2), we find that this compositional boundary is also coeval with the onset of the grand solar minimum (Fig. 3)
233 although the cause of this change is difficult to assess. In fact, Ti_{clr} as well as ln(Si/Ti) and ln(Ca/Ti), generally
234 regarded by Martin-Puertas et al. (2017) as indicating relative changes of biogenic silica concentrations and
235 authigenic calcite precipitation, are significantly correlated to the new [10]Be concentration measurements, but
236 also to the GRIP [10]Be data and to ^{14}C atmospheric production rate (Fig. 5 and Sup. Fig. 1). Because GRIP [10]Be
237 concentrations and ^{14}C atmospheric production rate are unaffected by environmental changes at MFM, we
238 suggest that the catchment area of MFM was likely influenced by the substantial changes in solar activity that
239 characterized this period rather than [10]Be concentration at MFM being affected by this sediment compositional
240 change. In support to this assumption, Czymzik et al. (2016) also reported negligible climate influences on [10]Be
241 deposition at MFM, even across distinct climatological boundaries. It can also be seen that the second and
242 smaller increase in varve thickness and Ti_{clr} is coeval with a second dip in solar activity shortly after 11,100
243 years BP (Fig. 3a and 3e). Finally, it is worthwhile to note that the percentage values of *Pinus* pollen, biogenic
244 silica, as well as pollen concentrations in MFM all decreased at 11,230-11,250 years BP while percentage values
245 of *Betula* increased (Brauer et al., 1999). Although not interpreted by the authors, these changes echo the
246 findings of Björck et al. (1997) who defined the PBO in terrestrial records of Sweden with a similar decrease of
247 pollen concentrations and more notably of *Pinus* pollen percentages, interpreted as a set-back of tree vegetation
248 in Southern Sweden. It should be stressed here that we cannot directly compare the palynology of MFM to these
249 Swedish lakes because of the challenging interpretation of the former record as well as the chronology
250 uncertainties and vicinity to the retreating Fennoscandian Ice Sheet of the latter records.

251 In summary, the radionuclide-based synchronization of the GICC05 and MFM2012 time-scales indicate
252 a combined timing offset of up to 98 (+33/-21) years during the earliest part of the Holocene. Correcting for this
253 offset, we observe that cold oscillations at both locations and inferred from water isotopes did not occur
254 simultaneously between 11,450 and 11,000 years BP. We further note that this pattern appears to be coupled
255 with large changes in solar activity, which leads us to suggest a causal link. More specifically, the cold and dry
256 climate oscillation in Greenland (the 11.4 ka event) occurred under a period of high solar activity between c.
257 11,370-11,270 years BP, but did not leave a discernable imprint in either varve thickness or biomarker δD from
258 MFM. Subsequently, solar activity dropped to a grand minimum that lasted for as long as 250 years. This change
259 was coeval with the termination of the 11.4 ka event (Greenland) and the onset of the MFM oscillation with
260 colder conditions inferred from δD data (Figs. 3d and 4). The ostensible link with solar activity which we infer
261 in view of Fig. 3 resembles what has been described substantially in the recent literature and is discussed in the
262 following section.

263

264 **4. 2 Solar forcing during 11,450-11,000 years BP**

265 Our suggestion of a causal sun-climate link during the earliest part of the Holocene can be further supported by
266 the spatial patterns of the 11.4 ka event in Greenland followed by a cold period at MFM starting at 11,250 years
267 BP (MFM oscillation). Based on our synchronization of the different paleoclimate records, we find an

268 asynchronous relationship between Greenlandic and European climate, characterized by cold and dry conditions
269 over Greenland, but with no evidence of it at MFM, under high solar activity and a warm and wetter Greenlandic
270 climate as well as a colder conditions at MFM for low solar activity (Fig. 3).

271   This pattern is consistent with a number of, but not all, climate modeling studies that find a top-down
272 influence of solar activity on North Atlantic/European atmospheric circulation patterns. This forcing mechanism
273 involves the increase in UV radiation during solar maxima years (Haigh et al., 2010; Lockwood et al., 2010)
274 which enhances the production of stratospheric ozone and leads to stratospheric heating through increased
275 absorption of long wave radiation (Haigh et al., 2010) especially at the equator. This increases the stratospheric
276 temperature gradient between the equator and poles (Simpson et al., 2009) leading to an acceleration of the polar
277 night jet (Kodera et al., 2002), which eventually propagates down to the troposphere via wave refraction
278 (Matthes et al., 2006; Ineson et al., 2011). In turn, this leads to patterns in surface pressure and temperature
279 which mimic those of the positive phase of the North Atlantic Oscillation in winter (Woollings et al., 2010;
280 Ineson et al., 2011). The opposite mode applies during periods of solar minima. It should however be stressed
281 that there is no consistent correlation between the NAO and solar forcing for the past centuries (Gray et al.,
282 2013; Ortega et al., 2015) although a solar influence on the region is not necessarily related to the NAO (Moffa-
283 Sánchez et al., 2014; Sjolte et al., 2018). Even though the spatial pattern we observe agrees well with a top-down
284 solar forcing, other mechanisms cannot be excluded to lie behind the different North-Atlantic response patterns.
285 Overall, it has to be kept in mind that different time periods with different climate boundaries could lead to
286 shifting atmospheric patterns.

287   In the following we explore the solar hypothesis further by investigating a modern analogue with
288 climate reanalysis data. Figure 6a shows the surface air temperature (SAT) anomalies in the North Atlantic
289 region for periods of solar maxima compared to periods of solar minima in 20CR (mean $\pm 1\sigma$ of the sunspot
290 group numbers from Svalgaard and Schatten (2016) between 1946-2011, see Sup. Fig. 2). It can be seen from
291 the SAT anomalies that a distinct antiphase pattern between Greenland and Europe is coincident with highs and
292 lows in solar activity. That is, Greenland experiences lower SATs during winters of solar maxima compared to
293 winters of solar minima whereas lower SATs are observed across Europe for winters of solar minima compared
294 to winters of solar maxima. This highlights the correspondence between the solar influence on North-Atlantic
295 climate which has been proposed to act during the 20th century and the synchronized climate proxy records
296 during the Early Holocene, in terms of spatial distribution of SAT anomalies. Furthermore, this correspondence
297 can also be qualitatively described by comparing the mean annual temperature anomalies at both Summit
298 (central Greenland) and MFM (Fig. 6c-d) throughout an average of all 11-year solar cycles of the 20th century
299 (Fig. 6b). Decadal temperature changes in 20CR at both Summit (blue curve in Fig. 6c) and MFM (red curve in
300 Fig. 6d) agree qualitatively well with centennial $\delta^{18}O$ and δD changes observed in Greenland ice cores and in
301 MFM sediments and during the period ranging from 11,450 to 11,000 years BP (black curves in Fig.6c-d, note
302 the different time-axes). Of specific interest here is the average transition from high to low solar activity that is
303 coincident with an annual temperature rise/drop of ca. 1K at Summit/MFM. Assuming changes in water isotopes
304 to be, in part, indicative of regional temperature changes (Dansgaard, 1964; Masson-Delmotte et al., 2005; Rach
305 et al., 2014; Fig. 4), this decadal pattern between Summit and MFM in climate reanalysis data mimics the
306 centennial-scale climate changes that prevailed in Greenland and Europe throughout 11,450-11,000 years BP.
307 Water isotopes are often dominated by a particular seasonal signal. It is therefore of interest to note that the

spatial patterns observed in climate reanalysis is also present during the summer, although to a lesser degree (Sup. Fig. 3).

It should be noted that the efficiency of the top-down mechanism remains largely unexplored for centennial time-scales. For instance, previous studies have proposed a top-down solar influence on atmospheric circulation on similar time-scales for both Greenland (Adolphi et al., 2014) and MFM (Martin-Puertas et al., 2012b) leading to a similar spatial pattern in reanalysis data. The modeling results in these studies do however only investigate the effect of decadal (11-years) changes in solar activity. In contrast, it was also shown more recently that the centennial response of North-Atlantic atmospheric circulation to solar forcing is correlated to the second mode of atmospheric circulation, the Eastern Atlantic Pattern, rather than to the first mode, the NAO (Sjolte et al., 2018). The latter study consequently does not find a similar pattern in SAT anomalies between Greenland and western Europe.

For the same reasons, another uncertainty arises from the relevance of using 20th century climate reanalysis as an analogy of Early Holocene conditions. In particular, the Laurentide ice sheet (LIS) is known to have played an important role in the position of the North Atlantic eddy-driven jet by accelerating and displacing it southward (Merz et al., 2015). However, it is also known that the LIS waned to the point of separation with the Cordilleran at about 14,000 years BP (Dyke, 2004). According to a study based on a transient climate simulation from the LGM (Löfverström and Lora, 2017), this separation led to a shift in the dominant topographic stationary wave source in North America. This, in turn, induced a transition from a strong and subtropical jet stream to a weaker and more meridionally tilted jet stream and storm track, as observed for present conditions. This suggests that similar atmospheric processes could have been at play during the earliest part of the Holocene, relative to today, in spite of different boundary conditions. Furthermore, the results from Fig. 6 arise from an 11-year solar cycle forcing which is considerably weaker and less persistent than the potential solar forcing that the 11,400 years BP solar maximum to 11,200 years BP grand solar minimum could have provoked, leading to possibly different reactions due to feedback processes. In fact, both the ^{14}C data and GRIP ^{10}Be data shown in Fig. 2 depict one of the most prominent increases of the Holocene record (Vonmoos et al., 2006), in terms of both amplitude and duration of the grand solar minimum. In comparison, its duration represents twice the length of the longest grand minimum known from sunspot observations (Svalgaard and Schatten, 2016) and called the Maunder minimum.

4.3 Solar-ocean coupling

The PBO has also been associated with an increase in freshwater supply hampering the Atlantic meridional overturning circulation (AMOC), possibly from the Baltic Ice Lake drainage and the rapidly waning Fennoscandian ice sheet (Björck et al., 1996; Hald and Hagen, 1998). It was next proposed by Fisher et al. (2002) that an outburst of Lake Agassiz could represent the trigger of the PBO through an increased thickness and extent of Arctic Ocean sea-ice pack. This would have resulted in an increased albedo as well as a slowdown of North Atlantic Deep Waters (NADW) formation due to increased freshwater delivery to the North Atlantic. However, the timing of the outburst event of which they attribute the PBO to (11,335 cal yr BP) has rather large uncertainties (± 130 to 230 years) due to the Δ^{14}C age plateau at this period. More recently, it was suggested that

346   even small changes in the prevalence of the AMOC can influence atmospheric circulation with couplings to the

347   NAO with an intensification of the former resulting in a negative index of the latter (Frankignoul et al., 2013).

348   To further investigate the potential spatial distribution of SAT anomalies due to a slowdown of the

349   AMOC, we again investigate 20CR for winters with a negative reconstructed AMOC index (Duchez et al., 2014)

350   compared to winters with a positive reconstructed AMOC index for the period 1961-2005 (Fig. 7a).

351   Interestingly, similar SAT anomalies subside as those for solar forcing. That is, an amplified meridional

352   temperature gradient with a colder Greenland and warmer western Europe are favoured in winters where the

353   AMOC is weaker, relative to winters where it is stronger. Although it is difficult to obtain direct evidence of an

354   AMOC slowdown during the Early Holocene, it is conceivable that the waning Fennoscandian ice sheet would

355   have released routinely enough freshwater to weaken and condition the AMOC for the onset of the 11.4 ka event

356   in Greenland. This result could also be explained by the influence of the NAO on the AMOC index, as it is

357   difficult to disentangle these tightly coupled processes (McCarthy et al., 2015). In this case, the persistent high

358   levels of solar activity, which also can favor such temperature and pressure patterns, could represent a potential

359   trigger for these climate oscillations. Figure 7b depicts the large temperature differences for winters where both

360   high solar activity and a weak AMOC prevailed during the period 1961-2005, with up to a -4K anomaly in

361   western Greenland. This however needs to be treated with caution due to the relatively short period of

362   observation that results in very few years where such solar activity and AMOC conditions existed in parallel

363   (Sup. Fig. 4).

364   In addition, a coupling between solar and freshwater forcing could also explain the lack of significant

365   climate responses to subsequent grand solar minima which were also large in amplitude but did not yield an

366   unequivocal impact on North Atlantic climate. It is indeed notable that the following changes in solar activity

367   occurred while the influence of freshwater release by the FIS was diminishing, and therefore the North Atlantic

368   was not conditioned as it was during the PBO. For instance, a similar but weaker event was found in the $\delta^{18}O$

369   signal of the GRIP ice core around 10,300 cal. years BP, coinciding with a low in $\Delta^{14}C$ (high solar activity) and

370   a cooling in the Faroe Islands (Björck et al., 2001). Whereas, the subsequent grand solar minimum which

371   occurred around 9,500 years BP (Vonmoos et al., 2006), at a time during which the FIS had completely vanished

372   (Stroeven et al., 2016), did not coincide with any evident climate oscillation in Greenland.

373   **5 Conclusions**

374   A comparison of new ^{10}Be concentration measurements from the varved Meerfelder Maar sediments covering

375   the period 11,310-11,000 years BP to the ^{10}Be data from the GRIP ice core in central Greenland showed a

376   combined offset of up to 98 (+33/-21) years between the MFM2012 and GICC05 chronologies. Correcting for

377   this offset allowed us to determine that the 11.4 ka event in Greenland has no coeval counterparts in Meerfelder

378   Maar and that it coincides with high solar activity. The time-scales synchronization also showed that an

379   environmental shift at MFM starting at 11,250 years BP is coincident with a transition from high solar activity to

380   a particularly long-lasting grand solar minimum as well as with the termination of the 11.4 ka event in

381   Greenland. The termination and onset of these cold oscillations in Greenland and then Meerfelder Maar are thus

382   synchronous with large changes in solar activity which is a pattern reproduced by a number of modeling studies.

383   Finally, we also postulate that a slowdown of the AMOC due to freshwater delivery from, for instance, the

Fennoscandian Ice Sheet could have served as a potential amplifier to this signal. The extent of the role that solar activity changes may have played on the climate of Greenland and Europe during the earliest part of the Holocene is unclear. This is due to the different boundary conditions which prevailed at the time compared to today but also to the proxy-evidence from MFM which is difficult to interpret. The main results from this study do however exemplify the usefulness of cosmogenic radionuclides to synchronize different paleo-records in an effort to investigate the timing and spatial distribution of past climate fluctuations with a high chronological precision.

Author contribution: FM performed the analysis in correspondence with RM, carried out the sampling with MC and CMP, and did the chemical preparation of the Meerfelder Maar [10]Be samples with help of AA while GP performed the measurements. FM wrote the manuscript. RM, MC, and FM initiated the project. FA provided the Bayesian synchronization and participated in the interpretation of climate reanalysis with JS. SB, AB, MC, and CMP assisted with the interpretation of the proxy data. All authors were involved in editing the manuscript.

Data availability: The new [10]Be data connected to this study have been submitted to the PANGAEA open access data library.

Competing interests: The authors declare that they have no conflict of interest.

Acknowledgements

This work was supported by the Royal Physiographic Society of Lund (grant to FM) and the Swedish Research Council (grant DNR2013-8421 to RM). MC was funded by a grant from the German Research Foundation (DFG grant CZ 227/4-1) and the BaltRap network of the Leibniz Association SAW-2017-IOW2). FA was supported by the Swedish research council (grant DNR2016-00218). ssAA thanks the UAEU for support through the UPAR funding. The authors would like to thank Inger Påhlsson for her help with the chemical preparation of the sediment [10]Be samples for AMS measurements.

References

Adolphi, F., and Muscheler, R.: Synchronizing the Greenland ice core and radiocarbon time-scales over the Holocene – Bayesian wiggle-matching of cosmogenic radionuclide records, Clim. Past, 12(1), 15–30, doi:10.5194/cp-12-15-2016, 2016.

Adolphi, F., Muscheler, R., Svensson, A., Aldahan, A., Possnert, G., Beer, J., Sjolte, J., Björck, S., Matthes, K. and Thiéblemont, R.: Persistent link between solar activity and Greenland climate during the Last Glacial Maximum, Nat. Geosci., 7(9), 662–666, doi:10.1038/ngeo2225, 2014.

Berggren, A.-M., Aldahan, A., Possnert, G., Haltia-Hovi, E. and Saarinen, T.: 10Be and solar activity cycles in varved lake sediments, AD 1900–2006, J. Paleolimnol., 44(2), 559–569, doi:10.1007/s10933-010-9437-1, 2010.

Bos, J. A. A., van Geel, B., van der Plicht, J. and Bohncke, S. J. P.: Preboreal climate oscillations in Europe: Wiggle-match dating and synthesis of Dutch high-resolution multi-proxy records, Quat. Sci. Rev., 26(15–16), 1927–1950, doi:10.1016/j.quascirev.2006.09.012, 2007.

Björck, S., Kromer, B., Johnsen, S., Bennike, O., Hammarlund, D., Lemdahl, G., Possnert, G., Rasmussen, T. L., Wohlfarth, B., Hammer, C. U. and Spurk, M.: Synchronized Terrestrial-Atmospheric Deglacial Records Around the North Atlantic, Science, 274(5290), 1155–60, doi:10.1126/SCIENCE.274.5290.1155, 1996.

Björck, S., Rundgren, M., Ingólfsson, Ó. and Funder, S.: The Preboreal oscillation around the Nordic Seas: terrestrial and lacustrine responses, J. Quat. Sci., 12(6), 455–465, doi:10.1002/(SICI)1099-1417(199711/12)12:6<455::AID-JQS316>3.0.CO;2-S, 1997.

Björck, S., Muscheler, R., Kromer, B., Andresen, C. S., Heinemeier, J., Johnsen, S. J., Conley, D., Koç, N., Spurk, M. and Veski, S.: High-resolution analyses of an early Holocene climate event may imply decreased solar forcing as an important climate trigger, Geology, 29(12), 1107, doi:10.1130/0091-7613(2001)029<1107:HRAOAE>2.0.CO;2, 2001.

Brauer, A., Endres, C., Günter, C., Litt, T., Stebich, M. and Negendank, J. F. W.: High resolution sediment and vegetation responses to Younger Dryas climate change in varved lake sediments from Meerfelder Maar, Germany, Quat. Sci. Rev., 18(3), 321–329, doi:10.1016/S0277-3791(98)00084-5, 1999.

Brauer, A., Endres, C., Zolitschka, B. and Negendank, J. F.: AMS radiocarbon and varve chronology from the annually laminated sediment record of Lake Meerfelder Maar, Germany. Radiocarbon, 42(3), 355-368, 2000.

Compo, G. P., Whitaker, J. S., Sardeshmukh, P. D., Matsui, N., Allan, R. J., Yin, X., Gleason, B. E., Vose, R. S., Rutledge, G., Bessemoulin, P., Brönnimann, S., Brunet, M., Crouthamel, R. I., Grant, A. N., Groisman, P. Y., Jones, P. D., Kruk, M. C., Kruger, A. C., Marshall, G. J., Maugeri, M., Mok, H. Y., Nordli, Ø., Ross, T. F., Trigo, R. M., Wang, X. L., Woodruff, S. D. and Worley, S. J.: The Twentieth Century Reanalysis Project, Q. J. R. Meteorol. Soc., 137(654), 1–28, doi:10.1002/qj.776, 2011.

Czymzik, M., Adolphi, F., Muscheler, R., Mekhaldi, F., Martin-Puertas, C., Aldahan, A., Oran Possnert, G. € and Brauer, A.: A varved lake sediment record of the [10]Be solar activity proxy for the Lateglacial-Holocene transition, Quat. Sci. Rev., 153, 31–39, doi:10.1016/j.quascirev.2016.10.007, 2016.

Czymzik, M., Muscheler, R., Adolphi, F., Mekhaldi, F., Dräger, N., Ott, F., Slowinski, M., Blaszkiewicz, M., Aldahan, A., Possnert, G. and Brauer, A.: Synchronizing [10]Be in two varved lake sediment records to IntCal13 ^{14}C during three grand solar minima, Clim. Past, 14(5), doi:10.5194/cp-14-687-2018, 2018.

Dansgaard, W.: Stable isotopes in precipitation, Tellus, 16(4), 436–468, doi:10.3402/tellusa.v16i4.8993, 1964.

Duchez, A., Hirschi, J. J.-M, Cunningham, S. A., Blaker, A. T., Bryden, H. L., De Cuevas, B., Atkinson, C. P., Mccarthy, G. D., Frajka-Williams, E., Rayner, D., Smeed, D. and Mizielinski, M. S.: A new index for the Atlantic Meridional Overturning Circulation at 26°N., J. of Clim., 27(17), 6439-6455, doi:10.1175/JCLI-D-13-00052.1, 2014.

Dyke, A. S.: An outline of North American deglaciation with emphasis on central and northern Canada, Dev. in Quat. Sci, 2, 373-424, doi.org/10.1016/S1571-0866(04)80209-4, 2004.

Finkel, R. C. and Nishiizumi, K.: Beryllium 10 concentrations in the Greenland Ice Sheet Project 2 ice core from 3-40 ka, J. Geophys. Res. Ocean., 102(C12), 26699–26706, doi:10.1029/97JC01282, 1997.

Fisher, T. G., Smith, D. G. and Andrews, J. T.: Preboreal oscillation caused by a glacial Lake Agassiz flood, Quat. Sci. Rev., 21(8–9), 873–878, doi:10.1016/S0277-3791(01)00148-2, 2002.

Frankignoul, C., Gastineau, G. and Kwon, Y. O.: The influence of the AMOC variability on the atmosphere in CCSM3, J. of Clim., 26(24), 9774-9790, doi.org/10.1175/JCLI-D-12-00862.1, 2013.

Gray, L. J., Scaife, A. A., Mitchell, D. M., Osprey, S., Ineson, S., Hardiman, S., Butchart, N., Knight, J., Sutton, R. and Kodera, K.: A lagged response to the 11 year solar cycle in observed winter Atlantic/European weather patterns, J. Geophys. Res. Atmos., 118(24), 13,405-13,420, doi:10.1002/2013JD020062, 2013.

Haigh, J. D., Winning, A. R., Toumi, R. and Harder, J. W.: An influence of solar spectral variations on radiative forcing of climate, Nature, 467(7316), 696–699, doi:10.1038/nature09426, 2010.

Hald, M. and Hagen, S.: Early Preboreal cooling in the Nordic seas region triggered by meltwater, Geology, doi:10.1130/0091-7613(1998)026<0615:EPCITN>2.3.CO;2, 1998.

Ineson, S., Scaife, A. A., Knight, J. R., Manners, J. C., Dunstone, N. J., Gray, L. J. and Haigh, J. D.: Solar forcing of winter climate variability in the Northern Hemisphere, Nat. Geosci., 4(11), 753–757, doi:10.1038/ngeo1282, 2011.

Kobashi, T., Severinghaus, J. P. and Barnola, J.-M.: 4 ± 1.5 °C abrupt warming 11,270 yr ago identified from trapped air in Greenland ice, Earth Planet. Sci. Lett., 268(3–4), 397–407, doi:10.1016/j.epsl.2008.01.032, 2008.

Kodera, K.: Solar cycle modulation of the North Atlantic Oscillation: Implication in the spatial structure of the NAO, Geophys. Res. Lett., 29(8), 59-1-59–4, doi:10.1029/2001GL014557, 2002.

Lane, C. S., Brauer, A., Martín-Puertas, C., Blockley, S. P. E., Smith, V. C. and Tomlinson, E. L.: The Late Quaternary tephrostratigraphy of annually laminated sediments from Meerfelder Maar, Germany, Quat. Sci. Rev., 122, 192-206, doi:10.1016/j.quascirev.2015.05.025, 2015.

Lockwood, M., Bell, C., Woollings, T., Harrison, R. G., Gray, L. J. and Haigh, J. D.: Top-down solar modulation of climate: evidence for centennial-scale change, Environ. Res. Lett., 5(3), 34008, doi:10.1088/1748-9326/5/3/034008, 2010.

Löfverström, M. and Lora, J. M.: Abrupt regime shifts in the North Atlantic atmospheric circulation over the last deglaciation, Geophys. Res. Lett., 44(15), 8047–8055, doi:10.1002/2017GL074274, 2017.

Magny, M., Vannière, B., de Beaulieu, J.-L., Bégeot, C., Heiri, O., Millet, L., Peyron, O. and Walter-Simonnet, A.-V.: Early-Holocene climatic oscillations recorded by lake-level fluctuations in west-central Europe and in central Italy, Quat. Sci. Rev., 26(15–16), 1951–1964, doi:10.1016/j.quascirev.2006.04.013, 2007.

Martin-Puertas, C., Brauer, A., Dulski, P. and Brademann, B.: Testing climate–proxy stationarity throughout the Holocene: an example from the varved sediments of Lake Meerfelder Maar (Germany), Quat. Sci. Rev., 58, 56–65, doi:10.1016/J.QUASCIREV.2012.10.023, 2012a.

Martin-Puertas, C., Matthes, K., Brauer, A., Muscheler, R., Hansen, F., Petrick, C., Aldahan, A., Possnert, G. and van Geel, B.: Regional atmospheric circulation shifts induced by a grand solar minimum, Nat. Geosci., 5(6), 397–401, doi:10.1038/ngeo1460, 2012b.

Martin-Puertas, C., Tjallingii, R., Bloemsma, M. and Brauer, A.: Varved sediment responses to early Holocene climate and environmental changes in Lake Meerfelder Maar (Germany) obtained from multivariate analyses of micro X-ray fluorescence core scanning data, J. Quat. Sci., 32(3), 427–436, doi:10.1002/jqs.2935, 2017.

Masson-Delmotte, V., Landais, A., Stievenard, M., Cattani, O., Falourd, S., Jouzel, J., Johnsen, S. J., Dahl-Jensen, D., Sveinsbjornsdottir, A., White, J. W. C., Popp, T. and Fischer, H.: Holocene climatic changes in Greenland: Different deuterium excess signals at Greenland Ice Core Project (GRIP) and NorthGRIP, J. Geophys. Res. Atmos., 110(D14), n/a-n/a, doi:10.1029/2004JD005575, 2005.

Matthes, K., Kuroda, Y., Kodera, K. and Langematz, U.: Transfer of the solar signal from the stratosphere to the troposphere: Northern winter, J. Geophys. Res., 111(D6), D06108, doi:10.1029/2005JD006283, 2006.

McCarthy, G. D., Haigh, I. D., Hirschi, J. J. M., Grist, J. P., and Smeed, D. A.: Ocean impact on decadal Atlantic climate variability revealed by sea-level observations, Nature, 521(7553), 508, doi:10.1038/nature14491, 2015.

Merz, N., Raible, C. C. and Woollings, T.: North Atlantic Eddy-Driven Jet in Interglacial and Glacial Winter Climates, J. Clim., 28(10), 3977–3997, doi:10.1175/JCLI-D-14-00525.1, 2015.

Moffa-Sánchez, P., Born, A., Hall, I. R., Thornalley, D. J. R. and Barker, S.: Solar forcing of North Atlantic surface temperature and salinity over the past millennium, Nat. Geosci., 7(4), 275–278, doi:10.1038/ngeo2094, 2014.

Muscheler, R., Beer, J., Wagner, G., Laj, C., Kissel, C., Raisbeck, G. M., Yiou, F. and Kubik, P. W.: Changes in the carbon cycle during the last deglaciation as indicated by the comparison of 10Be and 14C records, Earth Planet. Sci. Lett., 219(3–4), 325–340, doi:10.1016/S0012-821X(03)00722-2, 2004.

Muscheler, R., Kromer, B., Björck, S., Svensson, A., Friedrich, M., Kaiser, K. F. and Southon, J.: Tree rings and ice cores reveal 14C calibration uncertainties during the Younger Dryas, Nat. Geosci., 1(4), 263–267, doi:10.1038/ngeo128, 2008.

Muscheler, R., Adolphi, F. and Knudsen, M. F.: Assessing the differences between the IntCal and Greenland ice-core time scales for the last 14,000 years via the common cosmogenic radionuclide variations, Quat. Sci. Rev., 106, 81–87, doi:10.1016/J.QUASCIREV.2014.08.017, 2014.

Ortega, P., Lehner, F., Swingedouw, D., Masson-Delmotte, V., Raible, C. C., Casado, M. and Yiou, P.: A model-tested North Atlantic Oscillation reconstruction for the past millennium, Nature, 523(7558), 71–74, doi:10.1038/nature14518, 2015.

Pedro, J. B., Mcconnell, J. R., Van Ommen, T. D., Fink, D., Curran, M. A. J., Smith, A. M., Simon, K. J., Moy, A. D. and Das, S. B.: Solar and climate influences on ice core 10 Be records from Antarctica and Greenland during the neutron monitor era, Aust. Nucl. Sci. Technol. Organ., doi:10.1016/j.epsl.2012.08.038, 2012.

Rach, O., Brauer, a., Wilkes, H. and Sachse, D.: Delayed hydrological response to Greenland cooling at the onset of the Younger Dryas in western Europe, Nat. Geosci., 7(2), 109–112, doi:10.1038/ngeo2053, 2014.

Rasmussen, S. O., Andersen, K. K., Svensson, A. M., Steffensen, J. P., Vinther, B. M., Clausen, H. B., Siggaard-Andersen, M.-L., Johnsen, S. J., Larsen, L. B., Dahl-Jensen, D., Bigler, M., Röthlisberger, R., Fischer, H., Goto-Azuma, K., Hansson, M. E. and Ruth, U.: A new Greenland ice core chronology for the last glacial termination, J. Geophys. Res., 111(D6), D06102, doi:10.1029/2005JD006079, 2006.

Rasmussen, S. O., Vinther, B. M., Clausen, H. B. and Andersen, K. K.: Early Holocene climate oscillations recorded in three Greenland ice cores, Quat. Sci. Rev., 26(15–16), 1907–1914, doi:10.1016/j.quascirev.2007.06.015, 2007.

537   Rasmussen, S. O., Bigler, M., Blockley, S. P., Blunier, T., Buchardt, S. L., Clausen, H. B., Cvijanovic, I., Dahl-
538   Jensen, D., Johnsen, S. J., Fischer, H., Gkinis, V., Guillevic, M., Hoek, W. Z., Lowe, J. J., Pedro, J. B.,
539   Popp, T., Seierstad, I. K., Steffensen, J. P., Svensson, A. M., Vallelonga, P., Vinther, B. M., Walker, M. J.
540   C., Wheatley, J. J. and Winstrup, M.: A stratigraphic framework for abrupt climatic changes during the
541   Last Glacial period based on three synchronized Greenland ice-core records: refining and extending the
542   INTIMATE event stratigraphy, Quat. Sci. Rev., 106, 14–28, doi:10.1016/J.QUASCIREV.2014.09.007,
543   2014.

544   Reimer, P. J., Bard, E., Bayliss, A., Beck, J. W., Blackwell, P. G., Ramsey, C. B., Buck, C. E., Cheng, H.,
545   Edwards, R. L., Friedrich, M., Grootes, P. M., Guilderson, T. P., Haflidason, H., Hajdas, I., Hatté, C.,
546   Heaton, T. J., Hoffmann, D. L., Hogg, A. G., Hughen, K. A., Kaiser, K. F., Kromer, B., Manning, S. W.,
547   Niu, M., Reimer, R. W., Richards, D. A., Scott, E. M., Southon, J. R., Staff, R. A., Turney, C. S. M. and
548   van der Plicht, J.: IntCal13 and Marine13 Radiocarbon Age Calibration Curves 0–50,000 Years cal BP,
549   Radiocarbon, 55(4), 1869–1887, doi:10.2458/azu_js_rc.55.16947, 2013.

550   Seierstad, I. K., Abbott, P. M., Bigler, M., Blunier, T., Bourne, A. J., Brook, E., Buchardt, S. L., Buizert, C.,
551   Clausen, H. B., Cook, E., Dahl-Jensen, D., Davies, S. M., Guillevic, M., Johnsen, S. J., Pedersen, D. S.,
552   Popp, T. J., Rasmussen, S. O., Severinghaus, J. P., Svensson, A. and Vinther, B. M.: Consistently dated
553   records from the Greenland GRIP, GISP2 and NGRIP ice cores for the past 104 ka reveal regional
554   millennial-scale δ18O gradients with possible Heinrich event imprint, Quat. Sci. Rev., 106, 29–46,
555   doi:10.1016/J.QUASCIREV.2014.10.032, 2014.

556   Simpson, I. R., Blackburn, M., Haigh, J. D., Simpson, I. R., Blackburn, M. and Haigh, J. D.: The Role of Eddies
557   in Driving the Tropospheric Response to Stratospheric Heating Perturbations, J. Atmos. Sci., 66(5), 1347–
558   1365, doi:10.1175/2008JAS2758.1, 2009.

559   Sjolte, J., Sturm, C., Adolphi, F., Vinther, B. M., Werner, M., Lohmann, G. and Muscheler, R.: Solar and
560   volcanic forcing of North Atlantic climate inferred from a process-based reconstruction, Clim. Past, 14,
561   1179–1194, doi:10.5194/cp-14-1179-2018, 2018.

562   Southon, J.: A First Step to Reconciling the GRIP and GISP2 Ice-Core Chronologies, 0–14,500 yr B.P., Quat.
563   Res., 57(1), 32–37, doi:10.1006/qres.2001.2295, 2002.

564   Steig, E.J., Grootes, P.M. and Stuiver, M.: Seasonal Precipitation Timing and Ice Core Records. Science, 266,
565   1885–1886, doi.org/10.1126/science.266.5192.1885, 1994.

566   Stroeven, A. P., Hättestrand, C., Kleman, J., Heyman, J., Fabel, D., Fredin, O., Goodfellow, B. W., Harbor, J.
567   M., Jansen, J. D., Olsen, L., Caffee, M. W., Fink, D., Lundqvist, J., Rosqvist, G. C., Strömberg, B. and
568   Jansson, K. N.: Deglaciation of Fennoscandia, Quat. Sci. Rev., 147, 91–121,
569   doi:10.1016/J.QUASCIREV.2015.09.016, 2016.

570   Stuiver, M. and Polach, H. A.: Discussion Reporting of 14C Data, Radiocarbon, 19(3), 355–363,
571   doi:10.1017/S0033822200003672, 1977.

572   Svalgaard, L. and Schatten, K. H.: Reconstruction of the Sunspot Group Number: The Backbone Method, Sol.
573   Phys., 291(9–10), 2653–2684, doi:10.1007/s11207-015-0815-8, 2016.

574   Svensson, A., Andersen, K. K., Bigler, M., Clausen, H. B., Dahl-Jensen, D., Davies, S. M., Johnsen, S. J.,
575   Muscheler, R., Parrenin, F., Rasmussen, S. O., Röthlisberger, R., Seierstad, I., Steffensen, J. P. and

Vinther, B. M.: A 60 000 year Greenland stratigraphic ice core chronology, Clim. Past, 4, 47–57, doi.org/10.5194/cp-4-47-2008, 2008.

van der Plicht, J., van Geel, B., Bohncke, S. J. P., Bos, J. A. A., Blaauw, M., Speranza, A. O. M., Muscheler, R. and Björck, S.: The Preboreal climate reversal and a subsequent solar-forced climate shift, J. Quat. Sci., 19(3), 263–269, doi:10.1002/jqs.835, 2004.

Vinther, B. M., Clausen, H. B., Johnsen, S. J., Rasmussen, S. O., Andersen, K. K., Buchardt, S. L., Dahl-Jensen, D., Seierstad, I. K., Siggaard-Andersen, M.-L., Steffensen, J. P., Svensson, A., Olsen, J. and Heinemeier, J.: A synchronized dating of three Greenland ice cores throughout the Holocene, J. Geophys. Res., 111(D13), D13102, doi:10.1029/2005JD006921, 2006.

Vinther, B. M., Buchardt, S. L., Clausen, H. B., Dahl-Jensen, D., Johnsen, S. J., Fisher, D. A., Koerner, R. M., Raynaud, D., Lipenkov, V., Andersen, K. K., Blunier, T., Rasmussen, S. O., Steffensen, J. P. and Svensson, A. M.: Holocene thinning of the Greenland ice sheet, Nature, 461(7262), 385–388, doi:10.1038/nature08355, 2009.

von Grafenstein U., Erlenkeuser, H., Brauer, A., Jouzel, J. and Johnsen, S. J.: A mid-european decadal isotope-climate record from 15,500 to 5000 years B.P, Science, 284(5420), 1654–7, doi:10.1126/SCIENCE.284.5420.1654, 1999.

Vonmoos, M., Beer, J. and Muscheler, R.: Large variations in Holocene solar activity: Constraints from 10 Be in the Greenland Ice Core Project ice core, J. Geophys. Res., 111(A10), A10105, doi:10.1029/2005JA011500, 2006.

White, J. W. C., Barlow, L. K., Fisher, D., Grootes, P. M., Jouzel, J., Johnsen, S. J., Stuiver, M. and Clausen, H.B.: Stable isotope stacks from GRIP and GISP ice cores, https://doi.org/10.1594/PANGAEA.716878, 2009.

Woollings, T., Lockwood, M., Masato, G., Bell, C. and Gray, L.: Enhanced signature of solar variability in Eurasian winter climate, Geophys. Res. Lett., 37(20) doi:10.1029/2010GL044601, 2010.
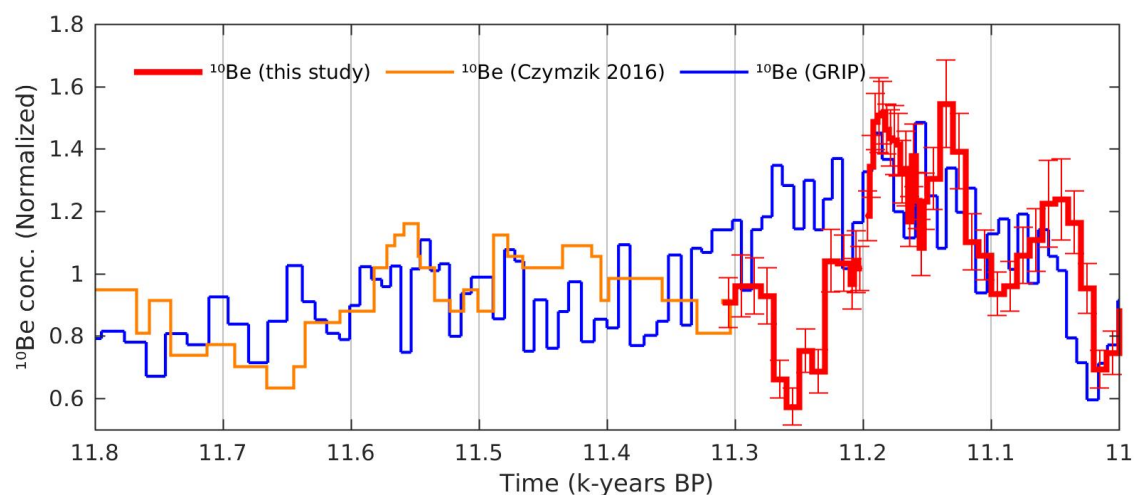
619
620
621
622
623
624
625
626
627
628
629
630 **Figure 1: The ¹⁰Be concentration data from Meerfelder maar (MFM), spanning the period 11,310-11,000 years BP are**
631 **plotted in red with corresponding measurement error bars. The record is completed in orange with the ¹⁰Be**
632 **measurements from the same sediment profile for the Late Glacial-Holocene transition (Czymzik et al., 2016). The**
633 **MFM ¹⁰Be data are plotted on the original MFM2012 chronology. The ¹⁰Be concentration data from the GRIP ice**
634 **core in central Greenland (Adolphi et al., 2014) is plotted in blue and on the GICC05 time-scale (Rasmussen et al.,**
635 **2006; Vinther et al., 2006; Svensson et al., 2008; Seierstad et al., 2014). All records have been normalized to their**
636 **mean.**

637
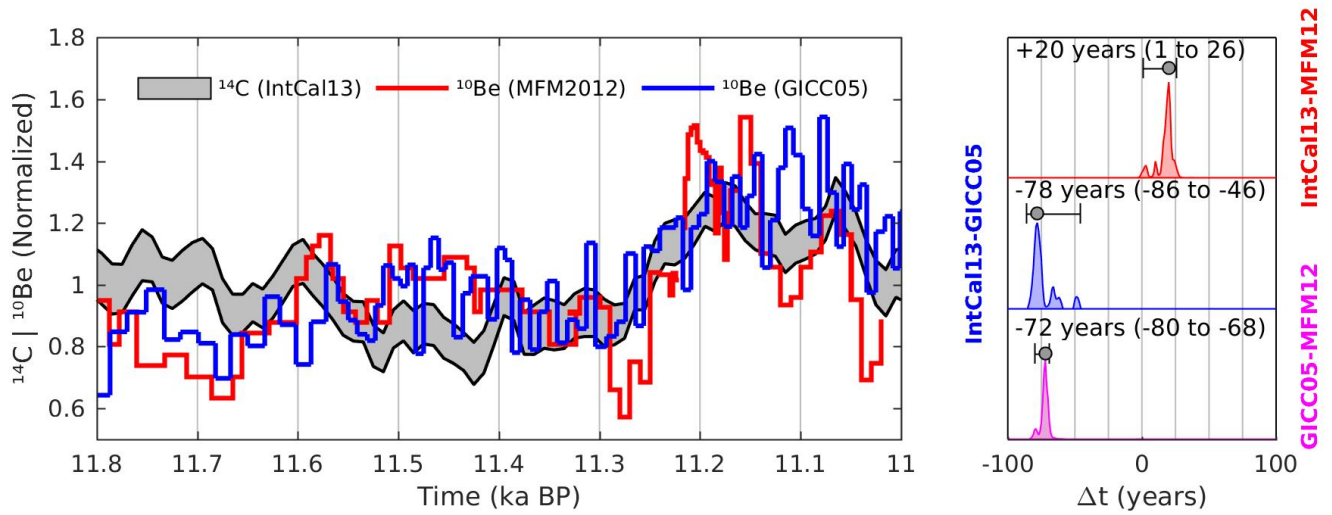
638
639 **Figure 2: Results from the Bayesian wiggle-matching of the different radionuclide records. The left panel shows both the**
640 **MFM ¹⁰Be data (in red) and the GRIP ¹⁰Be data (blue) once synchronized to the ¹⁴C production rate data inferred from the**
641 **IntCal13 calibration curve (1σ grey envelope). The right-hand panel displays the probability density functions for the best**
642 **fit between IntCal13-MFM2012 (in red), IntCal13-GICC05 (in blue) and GICC05-MFM2012 (in magenta), which resulted in**
643 **the synchronization in the left-hand panel and with a 95.4% confidence interval illustrated by the horizontal error bars.**

644
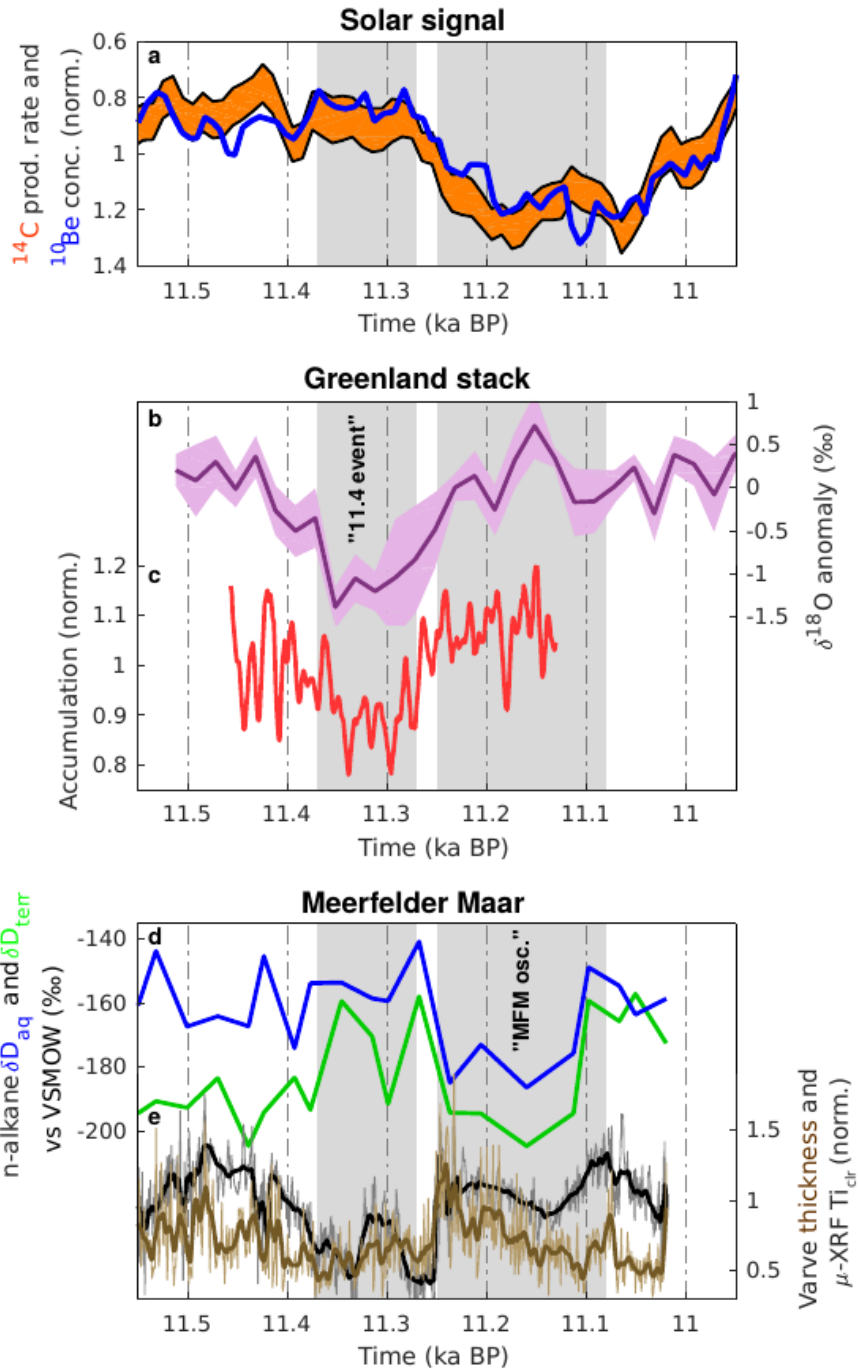
Figure 3: (a) ^{14}C production rate (orange envelope) and GRIP [10]Be data (blue) on a reversed y-axis to indicate variations in solar activity. (b) The $\delta^{18}O$ stack from the DYE-3, GRIP, NGRIP and Renland ice cores (Rasmussen et al., 2007; Vinther et al., 2009) is shown in magenta and (c) the modeled accumulation anomalies from Rasmussen et al. (2007) for DYE-3, GRIP, and NGRIP are shown in red. (d) The δD data record from lipid biomarkers of MFM sediments (Rach et al., 2014) is plotted in blue and green (aquatic and terrestrial) while (e) varve thickness (Martin-Puertas et al., 2012a) and varve μ-XRF Ti$_{clr}$ (Martin-Puertas et al., 2017) are plotted in brown and black, respectively. The grey bands depict the time of occurrence of the 11.4 ka event in Greenland and of the cold oscillation inferred from the MFM sediments (MFM oscillation). All data are plotted on the IntCal13 time-scale, as per Fig. 2.
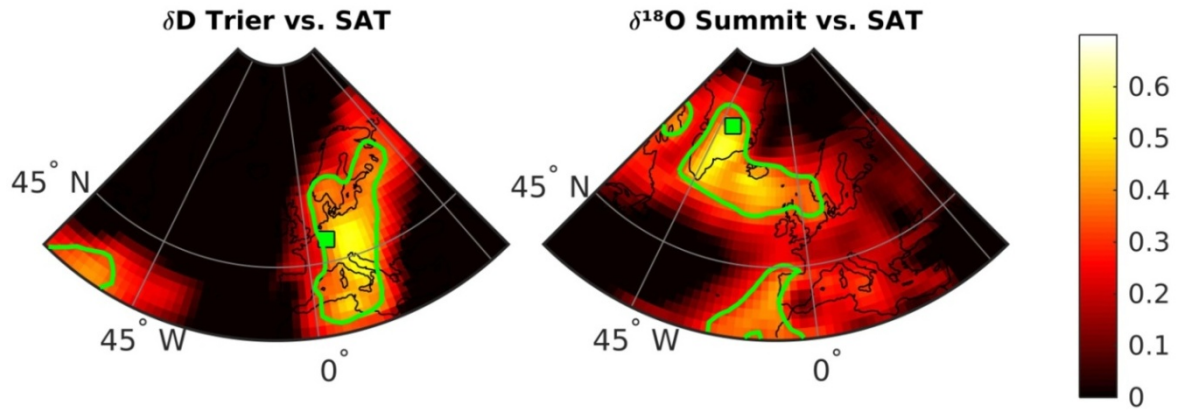
Figure 4: Left - Correlation map between annual δD in precipitation from the Trier station (green square – IAEA/WMO, 2016) and annual surface air temperatures in the NOAA-CIRES 20th climate reanalysis V2c (Compo et al., 2011) for the period AD 1978-2011. Right – Same as the left panel but for δ18O from the GISP2 ice core (green square – Steig et al., 1994; White et al., 2009) and for the period AD 1950-1986. Green contour lines represent significance levels for p < 0.1 (t-test). The difference in years selected arises from the different time-span of the δD and δ18O records used here.
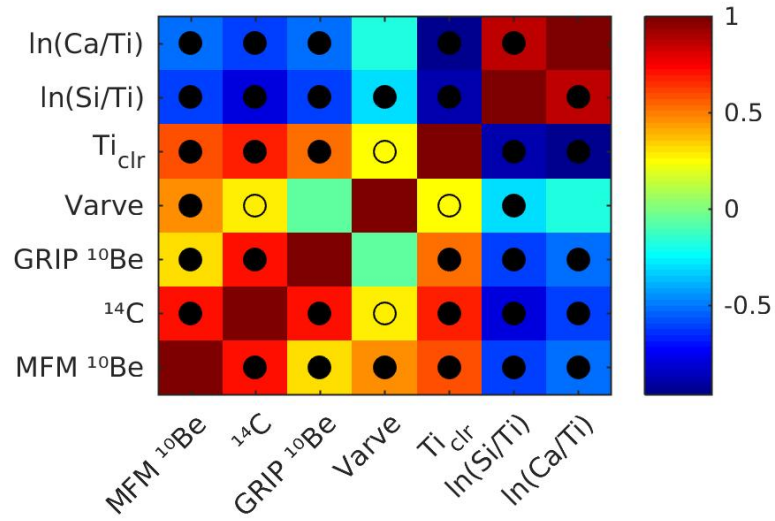
Figure 5: Color-coded correlation matrix between MFM ^{10}Be concentration, GRIP ^{10}Be concentration, ^{14}C production rate data, varve thickness, and μ-XRF data from MFM09 (Martin-Puertas et al., 2017). Open and filled circles denote significant correlations to the $p < 0.1$ and the $p < 0.05$ levels, respectively. All data were binned after the resolution of the MFM ^{10}Be concentration data for the period 11,310-11,000 years BP and a student t-test was performed to test the significance levels.
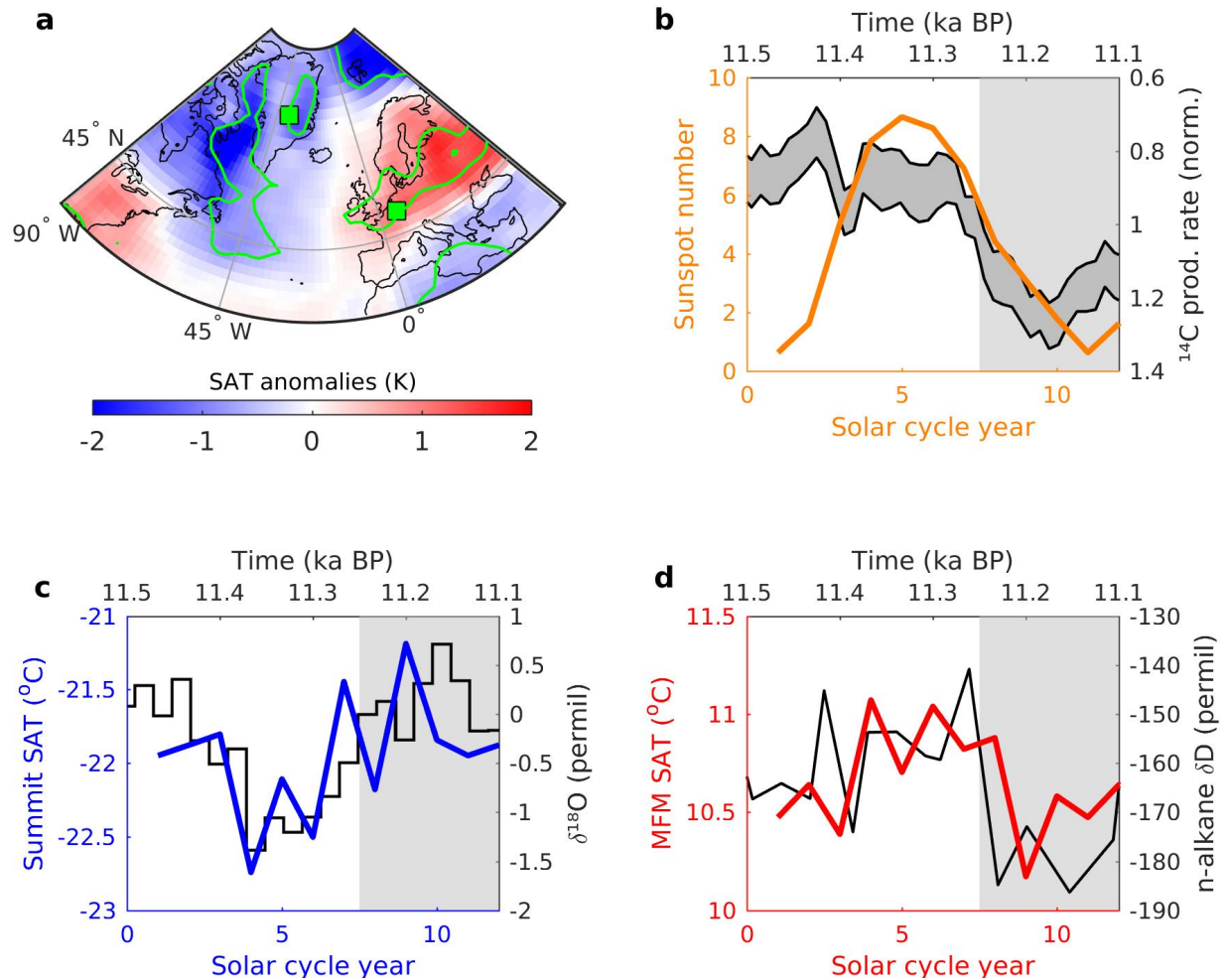
Figure 6: The 11.4 ka event and MFM oscillation compared to solar forcing of 20th century SAT in the North Atlantic region, as seen in 20CR. (a) Surface air temperature (SAT) anomalies for solar maxima winters (DJF) compared to solar minima winters (see Sup. Fig. 2) for the period 1946-2011 in 20th century climate reanalysis (Compo et al., 2011). The green squares point to the location of Summit and of MFM while the green contour lines represent significance levels for $p < 0.1$ (t-test). Years influenced by large tropical volcanic eruptions have been removed, as per Ineson et al. (2011). (b) The transition between high to low solar activity in the ^{14}C production rate data (grey envelope - top and right axes) compared to the mean sunspot group number of all 11-year solar cycles during 1900-2011 (orange curve - bottom and left axes). (c) The δ^{18}O stack (black curve - top and right axes) shown in Fig. 3b compared to the mean SAT at Summit (blue curve; bottom and left axes) throughout all 11-year solar cycles between 1900-2011 as in (b). (d) Same as (c) but with δD (black curve – top and right axes) and MFM SAT (red curve – bottom and left axes). Note the different time scale on the top (paleo records) and bottom axes (reanalysis data). The grey bands show the periods of low solar activity occurring on the two time periods that are compared.
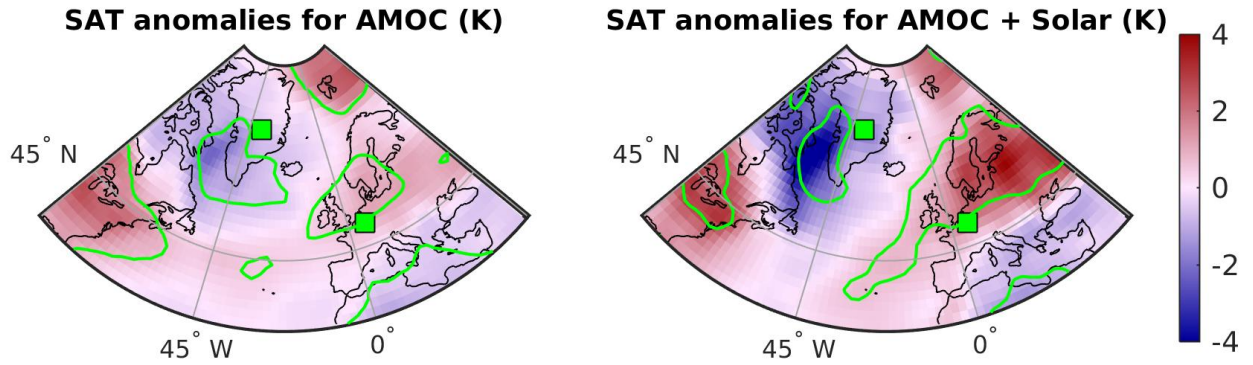
Figure 7: Left - Winter (DJF) surface air temperature anomalies for negative AMOC years compared to positive AMOC years for the period 1961-2005 in 20th century climate reanalysis (see Sup. Fig. 4). The green markers point to the location of Summit and of MFM while the green contour lines represent significance levels for p < 0.1 (t-test). Right - Same as left panel but for years of both negative AMOC and high solar activity.